

Tests of gauge boson couplings in polarized $e^- \gamma$ collisions

Martti Raidal

Research Institute for High Energy Physics,

P.O.Box 9, FIN-00014,

University of Helsinki

November 1994

Abstract

Single W -boson production in $e^- \gamma$ collisions with polarized beams is investigated. Helicity amplitudes for general couplings are derived and their properties are discussed. The results are applied to the Standard Model (SM) and the left-right model. In the framework of SM the updated estimates of the measurement precision of photon anomalous coupling parameters κ_γ , λ_γ at the NLC with $\sqrt{s_{ee}} = 500\text{GeV}$ are obtained. The production of right-handed gauge bosons W_2^- in these collisions is also analysed.

1 Introduction

In addition to the electron-positron option, the electron-electron and electron-photon collision modes of the Next Linear Collider (NLC) are also technically realizable [1]. During the recent years the physics potential of the latter options has been under intense study. While e^-e^- collisions have been found to be particularly suitable for the study of possible lepton number violating phenomena [2], the $e^-\gamma$ operation mode will also be well motivated from the point of view of new physics.

So far, the $e^-\gamma$ collisions have been studied using the photon spectrum of classical Bremsstrahlung. In the linear collider it will be possible to obtain high luminosity photon beams by backscattering intensive laser pulses off the electron beam [3] without considerable losses in the beam energy and with very high polarizability and monochromaticity [4]. This possibility makes the $e^-\gamma$ collisions well suited for testing the Higgs sector of the Standard Model (SM) [5], as well as for studying supersymmetric theories [6]. Moreover, the $e^-\gamma$ collision mode would be ideal for studying heavy gauge boson production processes [7, 8, 9], since the initial state photon provides us with a possibility to probe directly the gauge boson self-interactions.

In this paper we study a single massive vector boson production in $e^-\gamma$ collision,

$$e^-\gamma \rightarrow W^- N, \tag{1}$$

for any combination of beam polarization. Here W^- may stand for the ordinary SM charged vector boson W_1^- and N for the massless Dirac electron neutrino ν_e . However, we do not restrict ourselves only to this case, since a wide class of models beyond the SM predicts a existence of new heavy vector bosons and massive neutrinos. For example, in the left-right symmetric theory [10] based on the gauge group $SU(2)_R \times SU(2)_L \times U(1)_{B-L}$ the vector boson may also be a heavy right-handed

weak boson W_2 . There are two Majorana neutrinos in this model, which, in principle, can be mixed to give one heavy and one light mass eigenstate. The present lower limit for the mass of W_2 coming from TEVATRON is $M_{W_2} \geq 652$ GeV [11], so that the right-handed boson production will be kinematically forbidden in the initial phase of NLC, where the e^-e^+ center of mass energy is planned to be $\sqrt{s_{ee}} = 500$ GeV. At the final phase of NLC, however, reaction (1) could be kinematically allowed and favoured compared with, *e.g.*, the W_2 pair production in e^-e^+ collisions, since the mass of heavy Majorana neutrino could be smaller than the mass of W_2 . In the case of a sizeable mixing between the light, predominantly left-handed and the heavy, predominantly right-handed Majorana neutrinos the study of process (1) may extend the kinematical discovery range of W_2 almost up to the energy $\sqrt{s_{e\gamma}}$.

There are two Feynman diagrams contributing at the tree level to reaction (1) (see Fig. 1). One of them, the u-channel diagram, involves a triple gauge boson coupling making the process suitable for testing the non-Abelian gauge structure of the theory. A particularly interesting feature of process (1) is that it is sensitive *only* to the possible anomalous coupling of the photon, allowing one to discriminate between the photon anomalous coupling and the anomalous coupling of massive neutral gauge boson Z^0 . In a gauge theory the total cross section of reaction (1) approaches a constant value at high energies. Any deviation from the gauge form of the triple boson coupling would spoil the good high energy behaviour and lead to a violation of unitarity at some energy. At the energies of NLC these deviations are expected to be small, which will make their detection difficult. However, using polarized initial state particles one can enhance these effects.

In what follows we shall investigate reaction (1) for polarized beams taking into account the final state polarization measurements. We shall derive the helicity amplitudes assuming a general form of the relevant couplings and discuss their be-

behaviour, particularly at high energies and with anomalous couplings. We shall apply the general amplitudes in the case of two sample theories: the SM and the left-right model. We shall give an updated estimate for the precision of the anomalous triple boson coupling measurement at the first stage of NLC by analysing five different observables. We shall also study the discovery potential of the right-handed vector boson in the final phase of NLC via reaction (1).

The paper is organized as follows. In Section 2 we derive the helicity amplitudes and discuss the properties of the cross sections. In Section 3 we analyse the sensitivity of NLC to the triple boson coupling in the framework of the SM. In Section 4 we study reaction (1) in the case of the left-right model. A summary is given in Section 5.

2 Helicity amplitudes

In a gauge theory the transverse and longitudinal components of gauge bosons have different origins related to the different aspects of theory. The longitudinal components of massive vector bosons exist due to the Higgs mechanism, while the existence of the transverse components is dictated by the gauge invariance. Therefore, in order to obtain more information about the properties of gauge boson self-interactions, it would be useful to investigate reaction (1) by taking into account the polarization of particles. For this purpose we derive the helicity amplitudes of the process.

We do not restrict ourselves to any particular model but define the relevant couplings as general as possible. We assume that the charged current interaction is of the form

$$\mathcal{L}^{cc} = \frac{g}{2\sqrt{2}} \bar{N} \gamma_\mu (A + B\gamma_5) e W^{+\mu} + h.c., \quad (2)$$

where g is a coupling constant and A and B are parameters which allow us to choose

an arbitrary vector-axial-vector structure for the interaction. The parameters A and B enable us also to incorporate possible mixings of the particles.

The most general CP -conserving γWW interaction allowed by the electromagnetic gauge invariance is of the form [12]

$$\mathcal{L}_{\gamma WW} = -ie(W_{\mu\nu}^\dagger W^\mu A^\nu - W_\mu^\dagger A_\nu W^{\mu\nu} + \kappa_\gamma W_\mu^\dagger W_\nu F^{\mu\nu} + \frac{\lambda_\gamma}{M_W^2} W_{\tau\mu}^\dagger W_\nu^\mu F^{\nu\tau}), \quad (3)$$

where $W_{\mu\nu} = (\partial_\mu - ieA_\mu)W_\nu - (\partial_\nu - ieA_\nu)W_\mu$ and $F_{\mu\nu} = \partial_\mu A_\nu - \partial_\nu A_\mu$. The coefficients κ_γ and λ_γ are related to the magnetic moment μ_W and the electric quadrupole moment \mathcal{Q}_W of W according to

$$\begin{aligned} \mu_W &= \frac{e}{2M_W}(1 + \kappa_\gamma + \lambda_\gamma), \\ \mathcal{Q}_W &= -\frac{e}{M_W^2}(\kappa_\gamma - \lambda_\gamma). \end{aligned}$$

In a gauge theory at tree level the coefficients have the values $\kappa_\gamma = 1$ and $\lambda_\gamma = 0$.

In the case of the s-channel diagram we also need the $\gamma e^- e^-$ vertex, which is assumed to have the same form as in QED.

In our calculation we have neglected the electron mass. Accordingly, the longitudinally polarized electrons coincide with their left- and right-handed chirality states denoted by $\lambda = -\frac{1}{2}$ and $\lambda = \frac{1}{2}$, respectively. The electron momentum q is taken to be along the z-axis, $q^\mu = (|q|, 0, 0, |q|)$, and the momentum of the final state W^- is given by $k^\mu = (E_W, |k| \sin \theta, 0, |k| \cos \theta)$. We describe the polarized initial state photon by the polarization vectors

$$\epsilon_{photon}^\mu(k_1, \tau = \pm 1) = \frac{1}{\sqrt{2}}(0, \tau, -i, 0), \quad (4)$$

and the polarization states of the final state W^- by the polarization vectors

$$\epsilon_W^{\mu*}(k, \tau = \pm 1) = \frac{1}{\sqrt{2}}(0, -\tau \cos \theta, i, \tau \sin \theta),$$

$$\epsilon_W^{\mu*}(k, \tau = 0) = \frac{1}{\sqrt{M_W}}(|k|, E_W \sin \theta, 0, E_W \cos \theta). \quad (5)$$

The spinor \bar{u}_N , which describes a neutrino with mass M_N and momentum $p^\mu = (E_N, \vec{p})$, $\vec{p} = -\vec{k}$, is quantized with respect to the positive z-axis.

Now we write down the helicity amplitudes of process (1). Using the notation given above the helicity amplitudes can be written as

$$F_{\lambda\lambda'}^{\tau\tau'} = i \frac{eg(A + 2\lambda B)}{2\sqrt{2}} \bar{u}_N(p, \lambda') T_{\mu\nu} u_e(q, \lambda) \epsilon_{photon}^\nu(k_1, \tau) \epsilon_W^{\mu*}(k, \tau'), \quad (6)$$

where the tensor $T_{\mu\nu}$ is the sum of the two terms corresponding to the s- and u-channel diagrams. The first lower and the first upper indices in $F_{\lambda\lambda'}^{\tau\tau'}$ describe the polarization state of the electron and photon and the second pair describes the polarization states of the final state neutrino and W -boson, respectively. Tensor $T_{\mu\nu}$ is of the form

$$T_{\mu\nu} = \frac{\gamma_\mu (\not{q} + \not{k}) \gamma_\nu}{s} - \frac{1}{u - M_W^2} \left(\gamma^\rho - \frac{(\not{p}' - \not{q})(k_1 - k)^\rho}{M_W^2} \right) \Gamma_{\nu\mu\rho}, \quad (7)$$

where

$$\begin{aligned} \Gamma_{\nu\mu\rho} = & -2k_\nu g_{\mu\rho} - (1 + \kappa_\gamma - \lambda_\gamma) k_{1\mu} g_{\nu\rho} + (k + (\kappa_\gamma - \lambda_\gamma) k_1)_\rho g_{\mu\nu} \\ & + \frac{\lambda_\gamma}{M_W^2} (k + k_1)_\rho ((k \cdot k_1) g_{\mu\nu} - k_\nu k_{1\mu}), \end{aligned} \quad (8)$$

with $-ie\Gamma_{\nu\mu\rho}$ being the γWW vertex.

The amplitudes read as ($\lambda = \pm \frac{1}{2}$ and $\tau, \tau' = \pm 1$, longitudinal W 's are denoted by 0):

$$\begin{aligned} F_{\lambda\lambda'}^{\tau\tau'} = & -i \frac{eg}{8} (A + 2\lambda B) \sqrt{\sqrt{s}(E_N + M_N)} \left(\left(1 + \frac{|p|}{E_N + M_N} \right) \frac{(1 + 2\lambda\tau)(1 + \tau\tau')}{\sqrt{s}} \sin \frac{\theta}{2} \right. \\ & + \frac{\tau\tau'}{u - M_W^2} \left\{ \left(1 + \frac{|p|}{E_N + M_N} \right) \left[(G_2(1 + 2\lambda\tau') - G_1(1 + 2\lambda\tau)) \cos \frac{\theta}{2} - G_3 \sin \frac{\theta}{2} \right] \right. \\ & \left. \left. - \left(1 - \frac{|p|}{E_N + M_N} \right) G_4 \sin \frac{\theta}{2} \right\} \right), \end{aligned}$$

$$\begin{aligned}
F_{\lambda-\lambda}^{\tau\tau'} &= -i\frac{eg}{8}(A+2\lambda B)\sqrt{\sqrt{s}(E_N+M_N)}\left(\left(1-\frac{|p|}{E_N+M_N}\right)\frac{(1+2\lambda\tau)(\tau-\tau')}{\sqrt{s}}\cos\frac{\theta}{2}\right. \\
&\quad \left.+\frac{2\lambda\tau\tau'}{u-M_W^2}\left\{\left(1-\frac{|p|}{E_N+M_N}\right)\left[\left(G_1(1+2\lambda\tau)+G_2(1-2\lambda\tau')\right)\sin\frac{\theta}{2}-G_3\cos\frac{\theta}{2}\right]\right.\right. \\
&\quad \left.\left.-\left(1+\frac{|p|}{E_N+M_N}\right)G_4\cos\frac{\theta}{2}\right\}\right), \\
F_{\lambda\lambda}^{\tau 0} &= -i\frac{eg}{4\sqrt{2}M_W}(A+2\lambda B)\tau\sqrt{\sqrt{s}(E_N+M_N)}\left(\left(1+\frac{|p|}{E_N+M_N}\right)\frac{(1+2\lambda\tau)(E_W+|p|)}{\sqrt{s}}\cos\frac{\theta}{2}\right. \\
&\quad \left.-\frac{1}{u-M_W^2}\left\{\left(1+\frac{|p|}{E_N+M_N}\right)\left[G_1^0(1+2\lambda\tau)\cos\frac{\theta}{2}+(G_2(E_W+|p|)+G_3^0)\sin\frac{\theta}{2}\right]\right.\right. \\
&\quad \left.\left.+\left(1-\frac{|p|}{E_N+M_N}\right)G_4^0\sin\frac{\theta}{2}\right\}\right), \\
F_{\lambda-\lambda}^{\tau 0} &= -i\frac{eg}{4\sqrt{2}M_W}(A+2\lambda B)\sqrt{\sqrt{s}(E_N+M_N)}\left(\left(1-\frac{|p|}{E_N+M_N}\right)\frac{(1+2\lambda\tau)(E_W-|p|)}{\sqrt{s}}\sin\frac{\theta}{2}\right. \\
&\quad \left.+\frac{2\lambda\tau}{u-M_W^2}\left\{\left(1-\frac{|p|}{E_N+M_N}\right)\left[G_1^0(1+2\lambda\tau)\sin\frac{\theta}{2}+(G_2(E_W-|p|)-G_3^0)\cos\frac{\theta}{2}\right]\right.\right. \\
&\quad \left.\left.-\left(1+\frac{|p|}{E_N+M_N}\right)G_4^0\cos\frac{\theta}{2}\right\}\right), \tag{9}
\end{aligned}$$

where the factors G_i and G_i^0 are defined as:

$$\begin{aligned}
G_1 &= -\frac{1+\kappa_\gamma-\lambda_\gamma}{2}\sqrt{s}\sin\theta, \\
G_2 &= 2|p|\sin\theta, \\
G_3 &= \sqrt{s}\left\{(1+\kappa_\gamma-\lambda_\gamma)(\cos\theta-\tau\tau')+\frac{\lambda_\gamma}{M_W^2}\left[(M_W^2-u)(\cos\theta-\tau\tau')+\sqrt{s}|p|\sin^2\theta\right]\right\}, \\
G_4 &= -\frac{1-\kappa_\gamma+\lambda_\gamma}{2}\frac{M_N}{M_W^2}\left[(M_W^2-u)(\cos\theta-\tau\tau')+\sqrt{s}|p|\sin^2\theta\right], \\
G_1^0 &= -\frac{1+\kappa_\gamma-\lambda_\gamma}{2}\sqrt{s}(|p|+E_W\cos\theta), \\
G_3^0 &= \sqrt{s}\left\{-(1+\kappa_\gamma-\lambda_\gamma)E_W\sin\theta+\frac{\lambda_\gamma}{M_W^2}\left[(u-M_W^2)E_W+\sqrt{s}|p|(|p|+E_W\cos\theta)\right]\sin\theta\right\}, \\
G_4^0 &= -\frac{1-\kappa_\gamma+\lambda_\gamma}{2}\frac{M_N}{M_W^2}\sin\theta\left[(u-M_W^2)E_W+\sqrt{s}|p|(|p|+E_W\cos\theta)\right].
\end{aligned}$$

All the amplitudes are proportional to the factor $A+2\lambda B$ which makes the amplitudes vanish if the polarizations do not match with the chiral structure of the charged current interaction. In the amplitudes of type $F_{\lambda-\lambda}^{\tau\tau'}$ the flip of the neutrino helicity is controlled by the factor $(1-|p|/(E_N+M_N))$, which makes these amplitudes

vanish in the case of a massless neutrino. Because of the annihilation into a massless fermion, the s-channel contribution is nonzero only in the case when the electron and photon beams are similarly polarized.

In SM one has pure (V-A) current (*i.e.* $A = -B = 1$) and a massless Dirac neutrino, which fixes the electron and neutrino polarization states to $\lambda = -1/2$. If we assume a pure gauge model triple boson coupling then the amplitudes $F_{-\frac{1}{2}-\frac{1}{2}}^{-1+1}$ and $F_{-\frac{1}{2}-\frac{1}{2}}^{-1\ 0}$ vanish identically.

In the case of the left-right model there is also a (V+A) current (fixing $A = B = 1$ and $\lambda = 1/2$) in addition to the SM one and a massive Majorana neutrino. Again, without anomalous triple boson coupling, two of the helicity amplitudes, $F_{+\frac{1}{2}+\frac{1}{2}}^{+1-1}$ and $F_{+\frac{1}{2}-\frac{1}{2}}^{+1+1}$, vanish. Let us also note that the terms in the helicity amplitudes proportional to the neutrino mass, *i.e.* the terms with the coefficients G_4 and G_4^0 , are nonzero only if κ_γ and λ_γ differ from their gauge model values. This implies that the effects of the anomalous triple boson coupling are enhanced in the case of a massive neutrino compared with the massless case.

For determining the cross sections from the helicity amplitudes we have assumed 100% longitudinally polarized electron and linearly polarized photon beams. This is, of course, an approximation, since in practice the polarizations will never be ideal and one has to employ a density matrix giving the polarization parameters of the beams.

An interesting feature of reaction (1) is that in a gauge theory the total cross section for polarized beams is approaching a constant value,

$$\sigma \rightarrow \frac{e^2 g^2}{8\pi M_W^2}, \quad (10)$$

at high energies. The only contributions which remain in this limit are the ones corresponding to the case where the photon and W are both polarized the same way. The other terms decrease very rapidly with energy. For example, in the SM

both cross sections $\sigma_{-\frac{1}{2}-\frac{1}{2}}^{-1-1}$ and $\sigma_{-\frac{1}{2}-\frac{1}{2}}^{+1+1}$ approach the limit (10), which has a numerical value about 99pb, while $\sigma_{-\frac{1}{2}-\frac{1}{2}}^{+1-1}$ goes with energy as $1/s^3$ and $\sigma_{-\frac{1}{2}-\frac{1}{2}}^{+1-0}$ as $1/s^2$.

This good high energy behaviour will be violated if the triple boson coupling differs from its gauge model form. The cross section starts to increase with energy which leads to a contradiction with unitarity. At high energies both κ_γ and λ_γ terms in $\sigma_{-\frac{1}{2}-\frac{1}{2}}^{\pm 1-0}$ grow with energy as $\log s$ and in $\sigma_{-\frac{1}{2}-\frac{1}{2}}^{+1-1}$ as s if $\kappa_\gamma \neq 1$ and $\lambda_\gamma \neq 0$. The λ_γ terms in $\sigma_{-\frac{1}{2}-\frac{1}{2}}^{-1+1}$ increase also with s , while the cross sections $\sigma_{-\frac{1}{2}-\frac{1}{2}}^{\pm 1 \pm 1}$ are equal to a constant, which value depends only on κ_γ . However, these effects would still be quite small at the energies of NLC. Therefore, it is important to study the sensitivity of reaction (1) to the anomalous interaction taking into account the polarization effects.

3 Anomalous triple boson coupling in the Standard Model

The anomalous triple boson couplings have been theoretically well studied in e^+e^- collisions [12], and recently also the beam polarization has been taken into account in such studies [13]. Also the e^-e^- collisions have been found to be useful for this purpose [14]. One disadvantage of these collision processes is that they do not allow separate tests of the anomalous photon and Z^0 couplings since both γWW and ZWW vertices are involved in the reactions. The $e^- \gamma$ option to be offered by the NLC will be an ideal tool for studying the photon anomalous coupling separately.

In the context of the SM, the process (1) has already been investigated previously [7, 8, 15, 16], and its sensitivity to the photon anomalous coupling has been found to be comparable with the estimated sensitivity of the W pair production processes [8]. In this section we shall update these analysis for a 500 GeV e^+e^- collider, taking into account the effects of beam polarization and final state polarization as well as

the recent developments in the linear collider design.

The scattering of linearly polarized laser light off the electron beam produces a polarized photon beam with very hard spectrum strongly peaked at the maximum energy, which is about 84% of the electron beam energy [4]. The backscattered photon beam is slightly cone-shaped, where the hardest photons lie in the center and the softer components form the outer layers of the cone. In the $e^- \gamma$ collision the precisely collimated electron beam probes only the hardest photons of the γ beam making highly monochromatic collisions technically feasible¹. Therefore, we shall carry out our analysis for the center of mass energy $\sqrt{s_{e\gamma}} = 420$ GeV corresponding to the peak value of the photon spectrum, assuming that the small nonmonochromaticity effects of the photon beam will be treated separately in every particular experiment (similarly to the treatment of nonmonochromaticity of the electron beam due to the initial state Bremsstrahlung). The other relevant NLC parameters which we have used are the following:

- integrated luminosity $L_{int} = 100\text{fb}^{-1}$,
- the covering region of a detector $|\cos\theta| \leq 0.95$, which is already achieved in all LEP experiments,
- W^- reconstruction efficiency of 0.1.

The most straightforward and experimentally easiest observable for testing the parameters κ_γ and λ_γ is the differential cross section. Since in the SM the electron beam polarization is fixed by the handedness of the interaction ($A = -B = 1$), one can vary the initial state by choosing different photon beam polarization, $\tau_1 = \pm 1$. In order to minimize statistical and systematic errors it will be profitable to sum over the W^- polarization states. Similarly one can study the total cross section $\sigma_{\tau_1=\pm 1}^{tot}$.

¹The author thanks prof. V.Telnov for a clarifying discussion on this matter.

Since the differential cross sections are strongly peaked in the backward direction one would expect that also the forward backward asymmetries

$$A_{\pm}^{FB} = \frac{\sigma_{\tau_1=\pm 1}(\cos \theta \geq 0) - \sigma_{\tau_1=\pm 1}(\cos \theta \leq 0)}{\sigma_{\tau_1=\pm 1}(\cos \theta \geq 0) + \sigma_{\tau_1=\pm 1}(\cos \theta \leq 0)} \quad (11)$$

could be sensitive to the anomalous coupling. The fourth quantity, which reflects the effects of the beam polarization, is the polarization asymmetry A_{pol} defined as

$$A_{pol}(\cos \theta) = \frac{d\sigma_{\tau_1=+1} - d\sigma_{\tau_1=-1}}{d\sigma_{\tau_1=+1} + d\sigma_{\tau_1=-1}}. \quad (12)$$

We have also studied whether the measurement of the final state W -boson polarization could offer sensitive tests for κ_γ and λ_γ . The information about the polarization of W -boson can be obtained by measuring the angular distribution of its decay products. A suitable quantity would be the forward-backward asymmetry of the leptons produced in W^- decay, which is related to the cross sections corresponding to the different W^- polarization states $\tau_2 = \pm 1$ as follows (see *e.g.* ref.[15]):

$$\chi_{\pm}^{FB} = \frac{3}{4} \frac{\sigma_{\tau_1=\pm 1}^{\tau_2=-1} - \sigma_{\tau_1=\pm 1}^{\tau_2=+1}}{\sigma_{\tau_1=\pm 1}^{tot}}. \quad (13)$$

Let us now study numerically the sensitivity of these five quantities for determining the values of κ_γ and λ_γ in the NLC. We have carried out a χ^2 analysis by comparing the SM prediction of the observables with those corresponding to the anomalous κ_γ and λ_γ . All the contours are calculated at 90% confidence level, which corresponds to $\Delta\chi^2 = 4.61$. The statistical errors are computed assuming the NLC parameters given above. The systematic errors are estimated by assuming the uncertainty of the cross section measurement to be at the level of $\sim 2\%$ [17], coming mainly from the errors in the luminosity measurement, the acceptance, the background subtraction and the knowledge of branching ratios. For the asymmetries the systematic uncertainty corresponding to the luminosity measurement cancels and for them the total systematic error of the cross sections is taken to be 1.5%.

All the observables are first analysed separately and after this a combined analysis is performed. Both forward-backward asymmetries, $A_{\tau_1}^{FB}$ and $\chi_{\tau_1}^{FB}$, turned out to be several times less sensitive to the anomalous coupling than the other three observables and therefore we shall not present separate results for them.

In Fig. 2 we plot the allowed domains of the photon anomalous coupling on the $(\kappa_\gamma, \lambda_\gamma)$ plane, which are obtained by analysing the polarization asymmetry A_{pol} (contour *a*) and the total cross sections $\sigma_{\tau_1=\pm 1}^{tot}$ (contour *b*). The combined contour, resulting from these two, is denoted by *c*. As can be seen in Fig. 2, in this small region the total cross section is much more sensitive to the parameter κ_γ than to λ_γ . This result can be easily understood on the basis of our discussion in the last Section. The bulk of the cross section comes from the polarization states $\tau_1 = \tau_2 = \pm 1$, which makes them most sensitive to the anomalous coupling. Since $\sigma_{\tau_1=\pm 1}^{\tau_2=\pm 1}$ do not depend on λ_γ at high energies, but depend on κ_γ at all energies, the sensitivity to λ_γ is much less than to κ_γ . If the polarization asymmetry alone would allow us to measure κ_γ with the precision $|\Delta\kappa_\gamma| = 0.1$ and λ_γ with the precision about $|\Delta\lambda_\gamma| = 0.02$, the combined result were much more restrictive, giving an improvement by a factor of 2 in the λ_γ measurement and by a factor of 3 in the κ_γ measurement.

The most sensitive observable to the photon anomalous coupling is the differential cross section. The contours of allowed regions in $(\kappa_\gamma, \lambda_\gamma)$ space obtained from its analysis are plotted in Fig. 3. The curves for the different photon polarization states $\tau_1 = \pm 1$ are indicated in the figure. The contour resulting from the combined analysis is denoted by *a*. As can be seen from Fig. 3 the most stringent constraints for the anomalous coupling are obtained in the case of left-handedly polarized electron and right-handedly polarized photon beams. This is an expected result, since the s-channel diagram in Fig. 1 does not contribute in this case and the entire cross section comes from the u-channel diagram, which probes the triple boson coupling.

The resultant allowed domain for κ_γ and λ_γ obtained by combining the measurements of all five observables we have considered is denoted by b in Fig. 3. As compared with contour a the improvement achieved by performing the combined analysis of all observables is small, implying that the main constraints come from the measurements of the differential cross sections.

Summarizing, we have found out that by studying reaction (1) in the NLC with the assumed set of parameters, one could constrain the anomalous triple boson coupling parameters κ_γ and λ_γ to the following regions:

$$-0.008 \leq 1 - \kappa_\gamma \leq 0.009,$$

$$-0.01 \leq \lambda_\gamma \leq 0.005.$$

Comparison with the recent analysis [13] of the W^- pair production in e^-e^+ collisions with polarized beams indicates that the sensitivity of a $\sqrt{s} = 500$ GeV electron-positron collider to κ_γ is similar to the sensitivity of a $\sqrt{s_{e\gamma}} = 420$ GeV electron-photon collider (the results are complementary). The limits for parameter λ_γ would in contrast be more stringent in $e^-\gamma$ than in e^-e^+ collisions. Let us emphasize again, that the bounds from process (1) are independent of the parameters of ZWW coupling, probing the anomalous coupling of the photon only.

4 Single heavy vector boson production in left-right model

In this section we shall study a discovery potential of the final phase of NLC considering process (1) in the framework of the left-right model. The gauge boson in the reaction $e_R^-\gamma \rightarrow W_2^- N$ is a heavy right-handed gauge boson of the model, while the neutrino could be either a heavy right-handed neutrino or, in the case of a large

neutrino mixing angle, the ordinary light neutrino ν . However, the last possibility could still be very much suppressed.

In the left-right symmetric model there is a right-handed triplet Higgs field $(\Delta^{--}, \Delta^-, \Delta^0)$, which breaks the $SU(2)_R \times SU(2)_L \times U(1)_{B-L}$ symmetry down to the SM symmetry. The neutral member of the triplet obtains a vacuum expectation value v which is responsible for giving masses to the right-handed gauge bosons and heavy Majorana neutrinos. The mass relations are the following: $M_{W_2} = gv/\sqrt{2}$ and $M_N = 2hv$, where g is the gauge coupling constant of $SU(2)_R$ (we assume it to be equal to the SM gauge coupling g) and h is an unknown Yukawa coupling constant.

The general helicity amplitudes given in eq. (9) are applicable in this particular model if we set $A = B = 1$, *i.e.*, assume purely right-handed interaction. Then the electron beam should also be right-handedly polarized. Parameters κ_γ and λ_γ are assumed to have their gauge model value if not stated otherwise. In order to see the relative importance of different polarization states we present in Fig. 4 the angular distributions of the differential cross sections for all combinations of polarizations. In Fig. 4 (I) we plot the differential cross sections for the left-handedly polarized photon beam assuming the collision energy $\sqrt{s_{e\gamma}} = 1.5$ TeV, the gauge boson mass $M_{W_2} = 700$ GeV and the neutrino mass $M_N = 300$ GeV. In Fig. 4 (II) we plot the same for the right-handedly polarized photon beam. As the figures show, the final states with a left-handed neutrino are clearly suppressed. The main part of the cross section is again coming from the case where the photon and W^- are polarized in the same way. The other polarization combinations are somewhat suppressed for the right-handedly polarized photon beam. While in the SM *all* differential cross sections are peaked in the backward direction, in this case the distributions are more flat for many polarization states providing better possibilities for detecting

the anomalous photon coupling.

The mass dependence of the total cross section of the process $e_R^- \gamma \rightarrow W_2^- N$ can be seen in Fig. 5, where we plot the cross section as a function of W_2^- mass for the center of mass energy $\sqrt{s_{e\gamma}} = 1.5$ TeV assuming the left- (Fig. 5 (I)) and right-handedly (Fig. 5 (II)) polarized photon beams. The curves denoted by a and b correspond to the neutrino masses $M_N = 300$ GeV and $M_N = 600$ GeV, respectively. The cross sections are found to be reasonably large for almost the entire kinematically allowed mass region, decreasing faster with M_{W_2} for the $\tau_1 = 1$ photons. At low W_2 masses the difference between a and b curve is small but for heavy W_2 masses the cross section depends strongly on the neutrino mass. If $M_N \leq M_{W_2}$, reaction (1) enables us to study heavier vector bosons than what is possible in the W_2^- pair production in $e^- e^+$ or $e^- e^-$ collisions. The reaction would be even more useful in this respect if the mixing between the heavy and the light neutrino is large enough to give observable effects. In Fig. 6 we plot the cross section of the reaction $e_R^- \gamma \rightarrow W_2^- \nu$ for different photon polarizations assuming a vanishing mass of ν and the neutrino mixing angle of $\sin \theta_N = 0.05$. For this set of parameters the process should be observable up to W -boson mass $M_W = 1.2$ TeV.

In order to study how sensitive the single heavy vector boson production process (1) is to the photon anomalous coupling in the left-right model we have carried out the χ^2 analysis of the differential cross section. The contours of the allowed regions at 90% C.L. in $(\kappa_\gamma, \lambda_\gamma)$ space are plotted in Fig. 7 assuming the collision energy $\sqrt{s_{e\gamma}} = 1.5$ TeV, the boson mass $M_{W_2} = 700$ GeV and the NLC parameters given in Section 3. The resulting curve for the neutrino mass $M_N = 300$ GeV assuming unpolarized beams as well as the contours obtained for the right-handedly polarized electron and $\tau_1 = \pm 1$ polarized photon beams are indicated in the figure. The combined result obtained from the measurements with polarized initial states

is denoted by a . As one can see, the improvement in the sensitivity compared with the case of unpolarized beams is essential.

To study how the sensitivity to the anomalous coupling depends on the neutrino mass we have repeated the analysis for the neutrino mass $M_N = 600$ GeV (contour b in Fig. 7). Despite of the smaller cross section the sensitivity has not decreased significantly. This is a consequence of the G_4 terms in helicity amplitudes (9) which are proportional to the neutrino mass and nonzero only in the presence of anomalous triple boson coupling.

5 Summary

The Next Linear Collider will provide us with the possibility to study nearly monochromatic high energy $e^- \gamma$ collisions with any combination of polarizations. This option is particularly suitable for studying the massive gauge boson production, since the initial state photon probes directly the gauge boson self-interactions vertex γWW . We have derived the helicity amplitudes of the reaction $e^- \gamma \rightarrow W^- N$ assuming arbitrary particle masses and a general form of the interactions involved. We have used the general helicity amplitudes to analyse two theories: the Standard Model and the left-right symmetric model.

In the case of the Standard Model our numerical results concern the sensitivity of the first phase of NLC ($\sqrt{s_{ee}} = 500$ GeV) to the parameters of anomalous photon coupling κ_γ and λ_γ , taking into account the polarization of the particles. We have performed a combined χ^2 analysis of five observables, according to which the NLC will be able to constrain the anomalous coupling parameters at 90% C.L. to the region $-0.008 \leq 1 - \kappa_\gamma \leq 0.009$, $-0.01 \leq \lambda_\gamma \leq 0.005$.

The left-right symmetric model serves as a sample theory for studying the po-

tential of the final phase of NLC to discover a new heavy right-handed W_2 . The cross section of the reaction is found to be large and, since there is just one W_2 in the final state, the study of this process could significantly extend the kinematic region covered by the W -boson pair production. The effects of the photon anomalous coupling are found to be bigger for the higher neutrino masses, compensating the effects of smaller cross section in testing the gauge boson self-coupling parameters.

Acknowledgement. The author thanks Jukka Maalampi and Matts Roos for the helpful discussions and expresses his gratitude to Emil Aaltosen Säätiö, Wihurin Rahasto and Viro Säätiö for grants.

References

- [1] See *e.g.* , *Proc. of the Workshop on Physics and Experiments with Linear Colliders* (Saariselkä, Finland, September 1991), eds. R. Orava, P. Eerola and M. Nordberg (World Scientific, 1992), and *Proc. of the Workshop on Physics and Experiments with Linear Colliders* (Waikoloa, Hawaii, April 1993), eds. F.A. Harris, S.L. Olsen, S. Pakvasa and X. Tata (World Scientific, 1993).
- [2] See *e.g.* , F. Cuyper, K. Kolodziej and R. Rückl, preprint MPI-PhT/94-33, and references therein;
P. Helde, K. Huitu, J. Maalampi and M. Raidal, preprint HU-SEFT R 1994-09, and references therein.
- [3] I. Ginzburg, G. Kotkin, V. Serbo and V. Telnov, *Pizma ZhEFT* **34** (1981) 514 and *Nucl. Instrum. Methods* **205** (1983) 47.

- [4] V. Telnov, talks given in *Gamma-Gamma Collider Workshop* (Berkeley, USA, March 28-31, 1994) and *First Arctic Workshop on Future Physics and Accelerators* (Saariselkä, Finland, August 21-26, 1994), to appear in proceedings.
- [5] E. Boos *et. al.*, Phys. Lett. **B 273** (1991) 173;
 K. Hagiwara, I. Watanabe and P. Zerwas, Phys. Lett. **B 278** (1992) 187;
 K. Cheung, Phys. Rev. **D 48** (1993) 1035.
- [6] F. Cuypers, G.J. van Oldenborgh and R. Rückl, Nucl. Phys. **B 383** (1992) 45;
 K. Huitu, J. Maalampi and M. Raidal, Nucl. Phys. **B 420** (1994) 449.
- [7] A. Grau and J.A. Grifols, Nucl. Phys. **B 233**(1984) 375.
- [8] S.Y. Choi and F. Schrempp, Phys. Lett. **B 272** (1991) 149.
- [9] K. Cheung, Nucl. Phys. **B 403** (1993) 572;
 K. Cheung, S. Dawson, T. Han and G. Valencia, preprints UCD-94-6 and NUHEP-TH-94-2.
- [10] J.C. Pati and A. Salam, Phys. Rev. **D 10** (1974) 275;
 R.N. Mohapatra and J.C. Pati, Phys. Rev **D 11** (1975) 566, 2558;
 G. Senjanovic and R.N. Mohapatra, Phys. Rev. **D 12** (1975) 1502.
- [11] M. Pohl, talk given in *27-th Int. Conf. on HEP*, Glasgow, July 20-17, 1994, to appear in proceedings.
- [12] K.J.F. Gaemers and G.J. Gounaris, Z. Phys. **C 1** (1979) 159;
 J. Maalampi, D. Schildknecht and K.H. Schwartz, Phys. Lett. **B 166** (1986) 361 and M. Kuroda, J. Maalampi, K.H. Schwartz and D. Schildknecht, Nucl. Phys. **B 284** (1987) 271;

- K. Hagiwara, R.D. Peccei, D.Zeppenfeld and K.Hikasa, Nucl. Phys. **B 282** (1987) 253.
- [13] A.A. Likhoded *et. al.*, preprints IC/93/288 and UTS-DFT-93-22.
- [14] D. Choudhury and F. Cuypers, Phys. Lett. **B 325** (1994) 500 and preprint MPI-PhT/94-24.
- [15] E. Yehudai, Phys. Rev. **D 44** (1991) 3434.
- [16] O. Phillipson, Z. Phys. **C 54** (1992) 643.
- [17] M. Frank, P.Mätting, R. Settles and Z. Zeuner, in *Proc. of the Workshop "e⁺e⁻ Collisions at 500 GeV: The Physics Potential,"* ed. P.M. Zerwas (1991), DESY 92-123B.

This figure "fig1-1.png" is available in "png" format from:

<http://arxiv.org/ps/hep-ph/9411243v1>

This figure "fig1-2.png" is available in "png" format from:

<http://arxiv.org/ps/hep-ph/9411243v1>

This figure "fig1-3.png" is available in "png" format from:

<http://arxiv.org/ps/hep-ph/9411243v1>

This figure "fig1-4.png" is available in "png" format from:

<http://arxiv.org/ps/hep-ph/9411243v1>

This figure "fig1-5.png" is available in "png" format from:

<http://arxiv.org/ps/hep-ph/9411243v1>

This figure "fig1-6.png" is available in "png" format from:

<http://arxiv.org/ps/hep-ph/9411243v1>

This figure "fig1-7.png" is available in "png" format from:

<http://arxiv.org/ps/hep-ph/9411243v1>

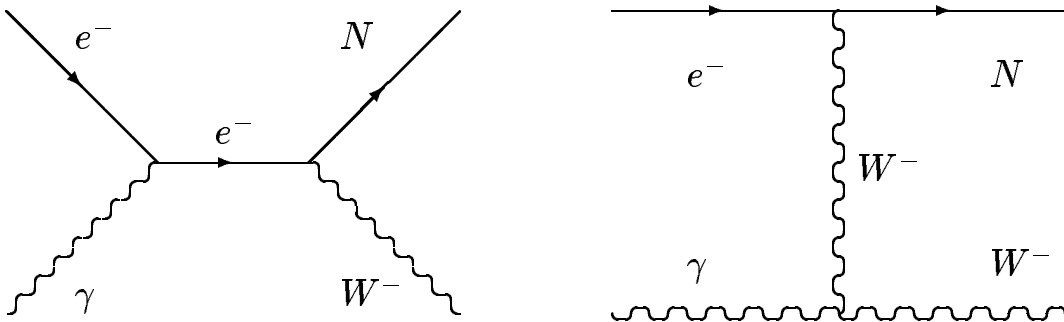


Figure 1: Feynman diagrams for the process $e^- \gamma \rightarrow W^- N$.

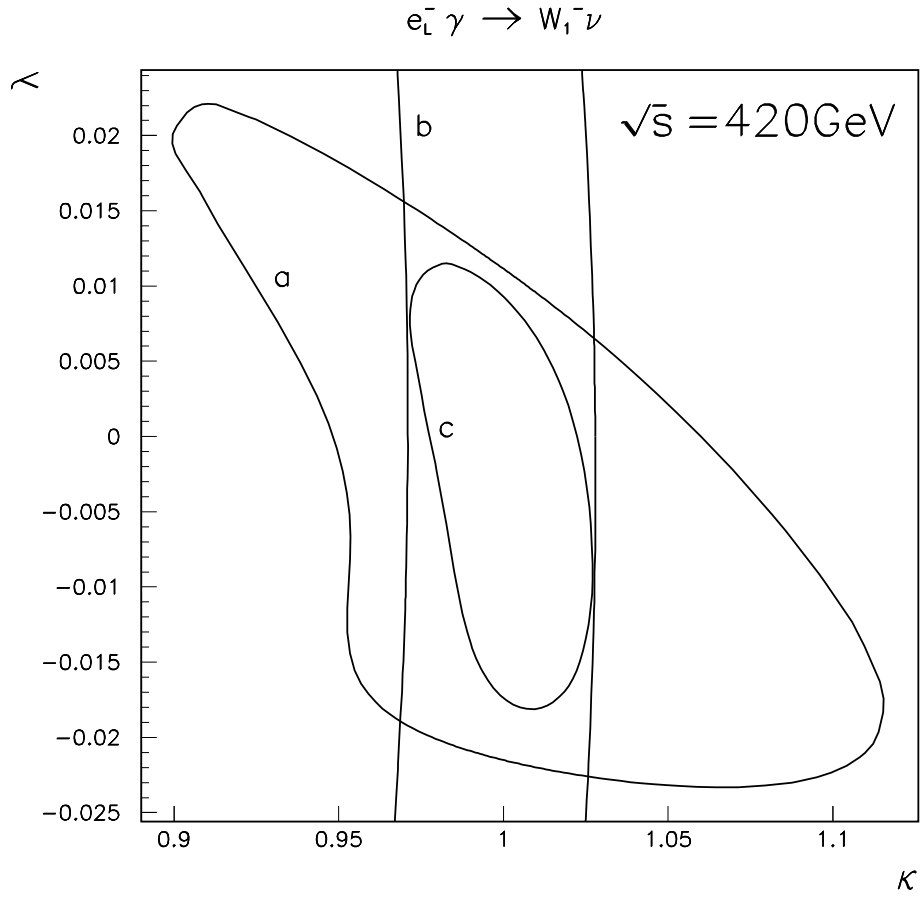


Figure 2: The allowed regions of the photon anomalous coupling parameters $\kappa_\gamma, \lambda_\gamma$ for the collision energy $\sqrt{s} = 420 \text{ GeV}$ in the framework of SM. The contours, obtained by analysing the polarization asymmetry and the total cross section, are denoted by a and b , respectively. The combined result of these two is denoted by c .

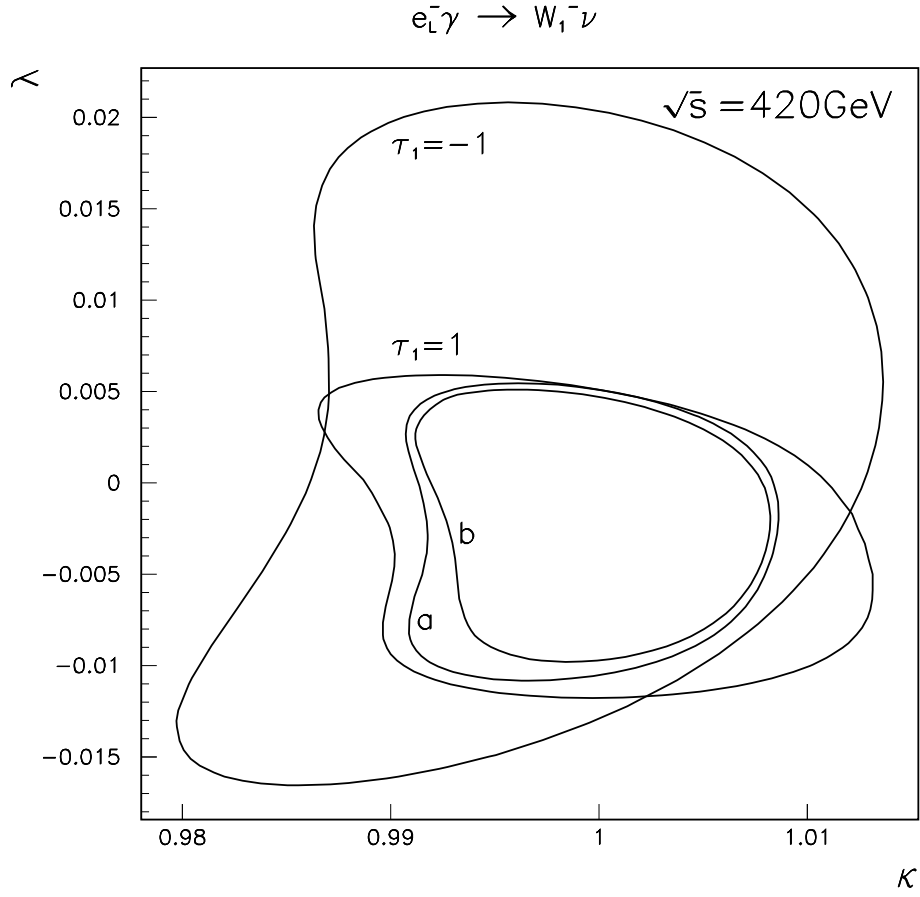


Figure 3: The allowed domains of the photon anomalous coupling parameters $\kappa_\gamma, \lambda_\gamma$ obtained by analysing the SM differential cross sections of different photon polarization states (as indicated on figure). The curve of combined analysis of the differential cross sections is denoted by a and the contour, resulting from the combined analysis of all five observables, is denoted by b .

$$e_R^- \gamma \rightarrow W_2^- N$$

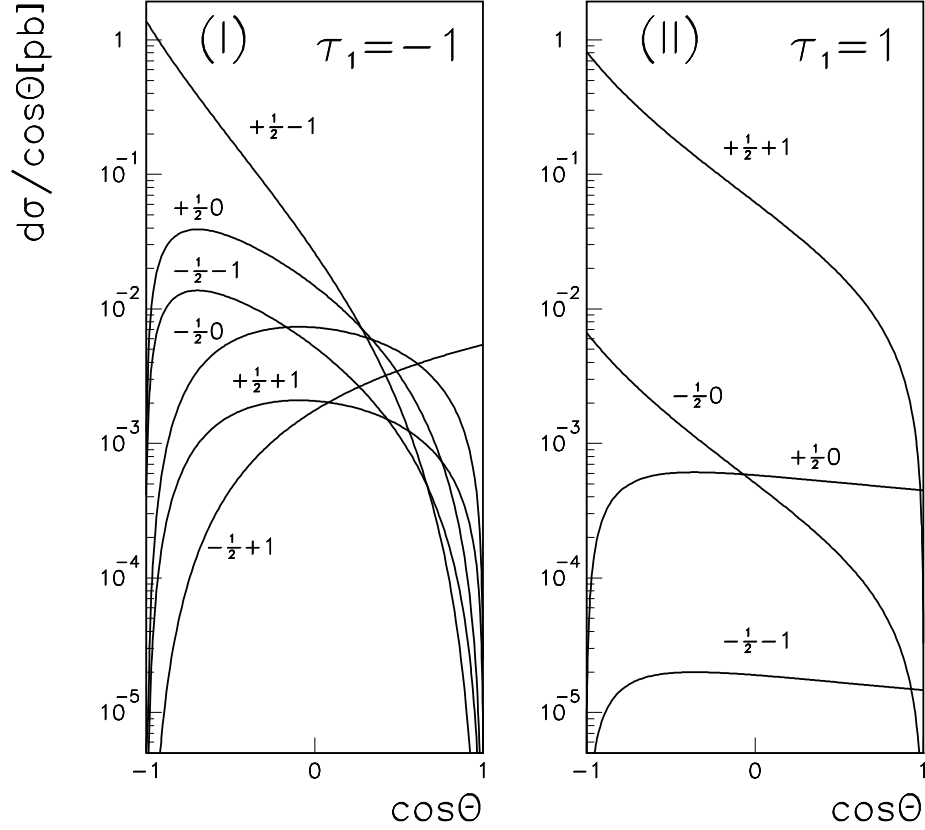


Figure 4: The angular distributions of differential cross sections of various NW_2^- polarization states for the left- (figure (I)) and right-handedly (figure (II)) polarized photon beams in the case of left-right model. The collision energy is taken to be $\sqrt{s_{e\gamma}} = 1.5\text{TeV}$, the mass of right handed vector boson $M_W = 700\text{GeV}$ and the mass of heavy neutrino $M_N = 300\text{GeV}$. The number pairs in figure denote the helicity states of neutrino and gauge boson, respectively.

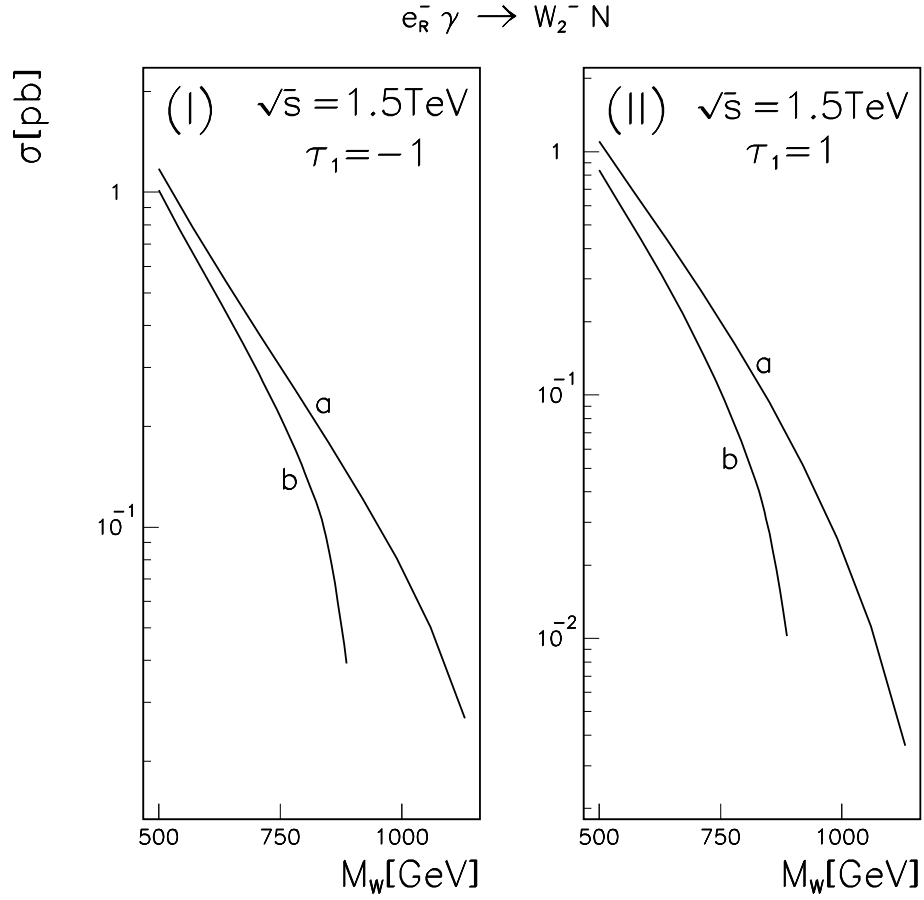


Figure 5: The total cross section of the process $e_R^- \gamma \rightarrow W_2^- N$ as a function of heavy gauge boson mass for the left- (figure (I)) and right-handedly (figure (II)) polarized photon beams. The collision energy is taken to be $\sqrt{s_{e\gamma}} = 1.5\text{TeV}$, the mass of right handed vector boson $M_W = 700\text{GeV}$ and the mass of heavy neutrino $M_N = 300\text{GeV}$ and $M_N = 600\text{GeV}$ for curves *a* and *b*, respectively.

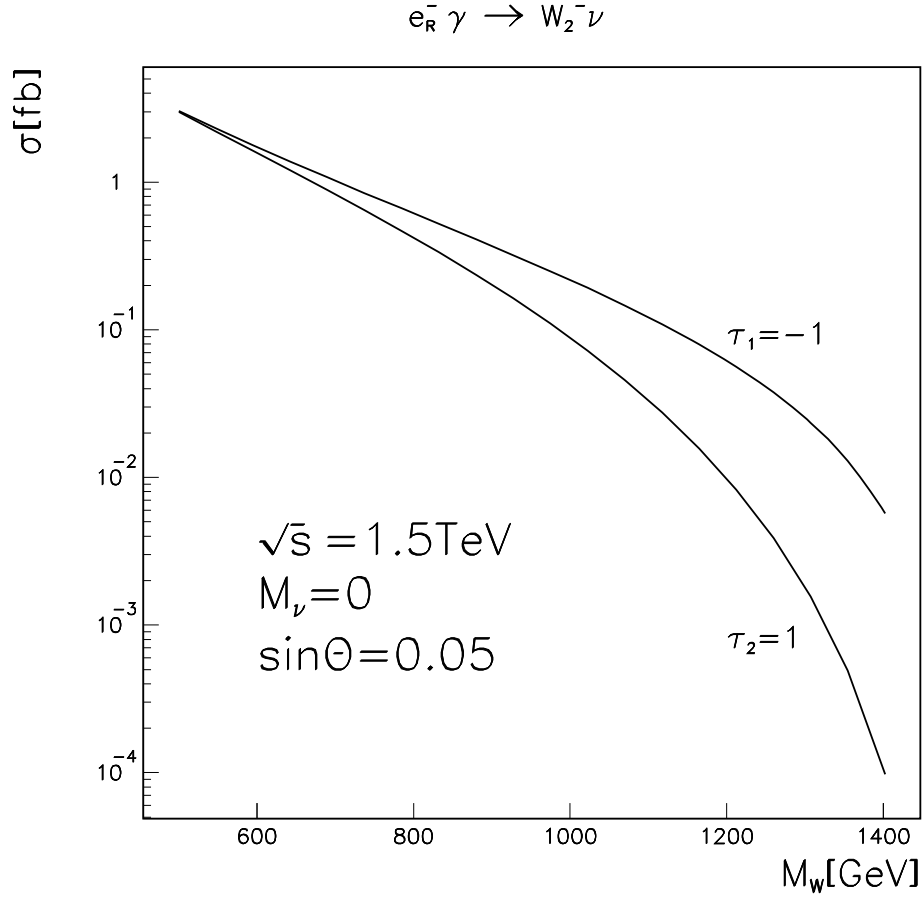


Figure 6: The total cross section of the process $e_R^- \gamma \rightarrow W_2^- \nu$ as a function of heavy gauge boson mass for the left- and right-handedly polarized photon beams. The collision energy is taken to be $\sqrt{s_{e\gamma}} = 1.5 \text{ TeV}$, the mass of right handed vector boson $M_W = 700 \text{ GeV}$ and the neutrino mixing angle $\sin \theta = 0.05$.

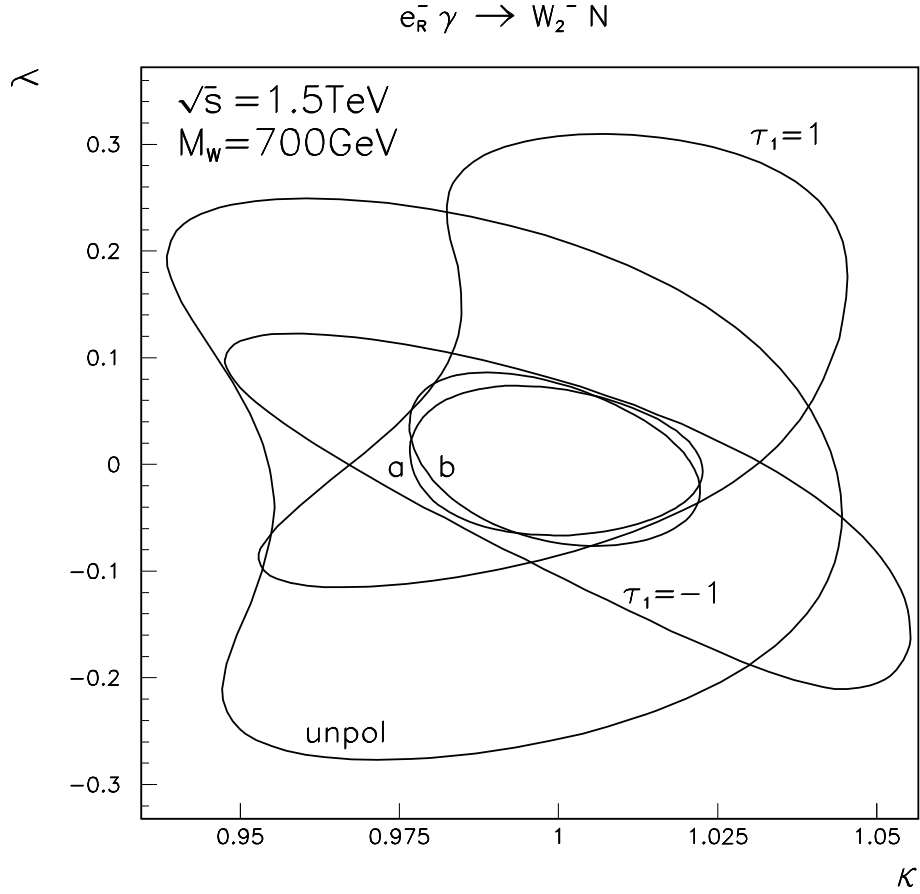


Figure 7: The allowed domains of the photon anomalous coupling parameters $\kappa_\gamma, \lambda_\gamma$ for the collision energy $\sqrt{s_{e\gamma}} = 1.5\text{TeV}$, the mass of right handed vector boson $M_W = 700\text{GeV}$ and the mass of heavy neutrino $M_N = 300\text{GeV}$, obtained from the analysis of differential cross section. The contours for unpolarized beams as well as for the right handed electron and differently polarized photon beams are indicated in the figure. The combined curve for the polarized beams is denoted by a , while the combined result in the case of heavy neutrino mass $M_N = 600\text{GeV}$ is denoted by b .